Signature Studies of Cosmic Magnetic Monopoles

Stuart D. Wick*,[1], Thomas W. Kephart†, and Thomas J. Weiler†

* *Department of Physics, University of Florida,*
Gainesville, FL 32611
†*Department of Physics and Astronomy, Vanderbilt University,*
Nashville, TN 37235

Abstract. This talk explores the possibility that the Universe may be populated with relic magnetic monopoles. Observations of galactic and extragalactic magnetic fields, lead to the conclusion that monopoles of mass $\lesssim 10^{14}$ GeV are accelerated in these fields to relativistic velocities. The relativistic monopole signatures and features we derive are (i) the protracted shower development, (ii) the Cherenkov signals, (iii) the tomography of the Earth with monopoles, and (iv) a model for monopole airshowers above the GZK cutoff.

INTRODUCTION

Any symmetry breaking, after inflation, of a semisimple group to a subgroup leaving an unbroken $U(1)$ may produce an observable abundance of magnetic monopoles. The inferred strength and coherence size of existing extragalactic magnetic fields suggest that any free monopole with a mass near or less than 10^{14} GeV would have been accelerated in magnetic fields to relativisitic velocities. On striking matter, such as the Earth's atmosphere, these relativistic monopoles will generate a particle cascade. Here we investigate the associated shower signatures.

The free monopole flux is limited only by Parker's upper bound $F_{\rm P} \sim 10^{-15}/\text{cm}^2/\text{s}/\text{sr}$ [1], which results from requiring that monopoles not short–circuit our Galactic magnetic fields faster than their dynamo can regenerate them. Since the Parker bound is several orders of magnitude above the observed highest–energy cosmic ray flux, existing cosmic ray detectors can meaningfully search for a monopole flux.

Because of their mass and integrity, a single monopole primary will continuously induce air–showers, in contrast to nucleon and photon primaries which transfer

---

[1]) Presenter at the First International Workshop on Radio Detection of High–Energy Particles, November 16 - 18, 2000, UCLA.

nearly all of their energy at shower initiation. Thus, the monopole shower is readily distinguished from non–monopole initiated showers. We also investigate the possibility that the hadronic cross–section of the monopole is sufficient to produce air–showers comparable to that from hadronic primaries, in which case existing data would already imply a meaningful limit on the monopole flux. One may even speculate that such monopoles may have been observed, as the primaries producing the enigmatic showers above the GZK cutoff at $\sim\ 5\ \times\ 10^{19}$ eV [2,3].

CHARACTERISTICS OF A MONOPOLE FLUX

The flux of monopoles emerging from a phase transition is determined by the Kibble mechanism [4]. At the time of the phase transition, roughly one monopole or antimonopole is produced per correlated volume, ξ_c^3. The resulting monopole number density today is

$$n_M \sim 10^{-19}\,(T_c/10^{11}\mathrm{GeV})^3(l_H/\xi_c)^3\,\mathrm{cm}^{-3}, \tag{1}$$

where ξ_c is the phase transition correlation length, bounded from above by the horizon size l_H at the time when the system relaxes to the true broken–symmetry vacuum. Although minimal $SU(5)$ breaking gives monopoles of mass $\sim 10^{17}$ GeV, there are ample theoretical possibilities for producing monopoles with smaller mass while maintaining the possibility of strong interaction cross–sections that avoid proton decay [5–8]. Based on the Kibble mechanism for monopole production, bounds on the universe's curvature constrain the monopole mass to less than 10^{13} GeV, while a comparison of the Kibble flux to the Parker limit constrains the monopole mass to less than 10^{11} GeV. The general expression for the relativistic monopole flux may be written [3]

$$F_M = c\,n_M/4\pi \sim 2\times 10^{-16}\,\left(\frac{M}{10^{11}\mathrm{GeV}}\right)^3\left(\frac{l_H}{\xi_c}\right)^3\,\mathrm{cm}^{-2}\,\mathrm{sec}^{-1}\,\mathrm{sr}^{-1}\,. \tag{2}$$

In higher dimensional cosmologies, the Kibble flux may be altered; then the straightforward Parker upper limit $F_P \leq 10^{-15}/\mathrm{cm}^2/\mathrm{sec}/\mathrm{sr}$ becomes the only reliable bound on the monopole flux. In the spirit of generality, we take the monopole mass M to be a free parameter and the Kibble mechanism is a rough guide to F_M. We require that F_M obey the Parker limit and assume that proton decay is avoided in a way that does not restrict the parameter M.

Monopole Structure

Monopoles are topological defects with a non-trivial internal structure; the core of the monopole is a region of restored unified symmetry. Monopoles are classified [4] by their topological winding, but for the case of GUT monopoles this classification is too coarse. In an $SU(5)$ GUT the fundamental minimally-charged monopole is six-fold degenerate. For an appropriate Higgs potential there are four other types of stable bound states formed from the fundamental monopoles [9,10]. This work distinguishes between those monopoles with color–magnetic charge and those with only ordinary $U_{EM}(1)$ magnetic charge. Thus, we adopt the nomenclature "q–monopoles" for those monopoles with color–magnetic charge and "l–monopoles" for those with only the ordinary magnetic charge.

The possible confinement of q–monopoles has recently been considered [11] via the formation of Z_3 color–magnetic "strings." If such a mechanism were realized one result could be the formation of color–singlet "baryonic–monopoles" in which the fusion of three differently colored strings produces a baryon–like composite of q–monopoles. The internal structure of a baryonic–monopole would approximate that of an ordinary baryon in the QCD string model, but with q–monopoles in the place of the quarks. Thus, the baryonic–monopole structure is quite different from a single l–monopole and, as such, it is shown to have a very different cross–section and cosmic ray shower profile.

Monopole Acceleration

The kinetic energy imparted to a magnetic monopole on traversing a magnetic field along a particular path is [3]

$$E_K = g \int_{\text{path}} \vec{B} \cdot \vec{dl} \sim g\, B\, \xi \sqrt{n} \tag{3}$$

where

$$g = e/2\alpha = 3.3 \times 10^{-8} \text{ esu} \quad (\text{or } 3.3 \times 10^{-8} \text{dynes/G}) \tag{4}$$

is the magnetic charge according to the Dirac quantization condition, B is the magnetic field strength, ξ specifies the field's coherence length, and $\sqrt{n}$ is a factor to approximate the random–walk through the n domains of coherent field traversed by the path. Galactic magnetic fields and magnetic fields in extragalactic sheets and galactic clusters range from about 0.1 to $100\mu G$, while their coherence lengths range from 10^{-4} to about 30Mpc [12,13]. These fields can accelerate a monopole from rest to the energy range 2×10^{20} to 5×10^{23} eV. For extragalactic sheets the number of random-walks can be roughly estimated to be of order $n \sim H_0^{-1}/50\,\text{Mpc} \sim 100$, and so $E_{\max} \sim 5 \times 10^{24}$ eV. Hence, monopoles with mass below $\sim 10^{14}$ GeV may be relativistic. The rest of this talk is devoted to the novel phenomenology of relativistic monopoles. As a prelude to calculating monopole signatures in various detectors, we turn to a discussion of the interactions of monopoles with matter.

RELATIVISTIC MONOPOLE ENERGY LOSS

Both l–monopoles and baryonic–monopoles are conserved in each interaction because of their topological stability. However, as conjectured above, their different internal structures will lead to differing shower profiles and signatures. Because of space limitations, in this talk we only consider the electromagnetic interactions of l–monopoles and the hadronic interactions of baryonic–monopoles.

The shower profile of baryonic–monopoles is based upon a model [14] where the hadronic cross–section grows after impact and the net energy transfer is enough to stop the monopole very quickly. Since this mechanism is model dependent, we consider the baryonic–monopole signatures less reliable. Further discussion of the baryonic–monopole is postponed until the final section.

Our most reliable signatures are for l–monopoles (which are referred to as "monopoles" for the remainder of this talk) and are based upon well understood electromagnetic processes. At large distances and high velocities, a monopole mimics the electromagnetic interaction of a heavy ion of charge $Z \sim 1/2\alpha \simeq 68$. We view the monopole as a classical source of radiation, while treating the matter–radiation interaction quantum mechanically. In this way, the large electromagnetic coupling of the monopole is isolated in the classical field, and the matter–radiation interaction can be calculated perturbatively.

Electromagnetic Interactions

We consider here the energy loss of a monopole resulting from four electromagnetic processes: collisions (ionization of atoms), e^+e^- pair production, bremsstrahlung, and the photonuclear interaction. All of these processes involve the scattering of a virtual photon, emitted by an incident monopole, off of a target particle.

The monopole–matter electromagnetic interaction for monopole boosts $\gamma < 100$ is well reported in the literature [15,16]. Previous works include atomic excitations and ionization losses, including the density suppression effect. These processes are collectively referred to as "collisional" energy losses and are $\propto \ln\gamma$. The pair production ($MN \to MNe^+e^-$) and bremsstrahlung ($MN \to MN\gamma$) energy losses are $\propto \gamma$, where M, N, e and γ represent a monopole, nucleus, electron, and photon respectively. The photonuclear ($MN \to MNX$, where X are hadrons) energy loss [17] is roughly $\propto \gamma^{1.28}$. For large γ, the pair production and photonuclear interactions dominate while bremsstrahlung is suppressed by the large monopole mass as M^{-1}. (By comparison, the bremsstrahlung of a muon is of similar strength to other radiative energy loss processes.)

Here we only have space to collect the electromagnetic energy loss processes together and plot them, in fig. (1), for $M = 100$ TeV monopoles (see [14] for more details).

MONOPOLE ELECTROMAGNETIC SIGNATURES

Signature events for monopoles are discussed with a specific emphasis on 1) the general shower development, 2) the direct Cherenkov signal, 3) the coherent radio–

Cherenkov signal, and 4) the tomography of the Earth's interior. Monopoles will be highly penetrating primaries, interacting via the electromagnetic force and all the while maintaining their structural integrity. On average, there will be a quasi-steady cloud of secondary particles traveling along with the monopole. Thus, we will call this type of shower "monopole–induced."

Given a fast monopole passing through matter, the various electromagnetic processes can inject energetic photons, electrons, positrons, and hadrons into the absorbing medium. If the energy of these injected secondary particles is sufficient (roughly greater than $E_c \sim 100$ MeV), they may initiate a particle cascade. In terms of the inelasticity $\eta \equiv \Delta E/E$, the condition for electromagnetic shower development is $\eta \gtrsim E_c/E_0 \simeq 10^{-12}\,(E_0/10^{20}\mathrm{eV})^{-1}$. Lower inelasticity events will contribute directly to ionization without intermediate particle production. The inelasticity per interaction and the subsequent shower development is best under-

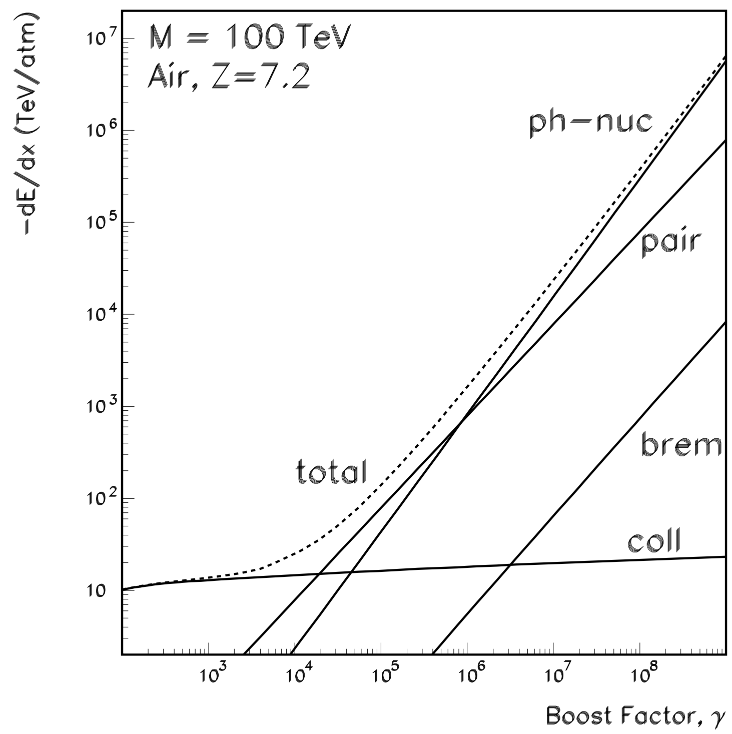

FIGURE 1. The electromagnetic energy loss from collisional, bremsstrahlung, electron–pair production, and the photonuclear interaction of a 100 TeV relativistic monopole in air. Collisional, pair production, and the photonuclear interaction are roughly independent of the monopole mass whereas bremsstrahlung is $\propto M^{-1}$. The units of energy loss are given in TeV per atmosphere.

stood for pair production. Detailed calculations [14] show that for $\gamma \gtrsim 10^4$ all of the monopole energy lost via pair production goes into the electromagnetic shower.

The contribution of the photonuclear process to the *electromagnetic* shower is indirect. The photonuclear interaction injects high energy hadrons into the monopole–induced shower. A subshower initiated by a high energy hadron will produce π^0's as secondaries, which each decay to 2 γ's. If these γ's have $E > E_c$, they may initiate an electromagnetic shower. So, only a fraction the energy lost via the photonuclear interaction contributes to the electromagnetic shower in the end.

Given the arguments above, it is reasonable to assume that pair production alone provides a lower bound to the electromagnetic shower size and that the pair production plus photonuclear interaction provides an upper bound. We plot the

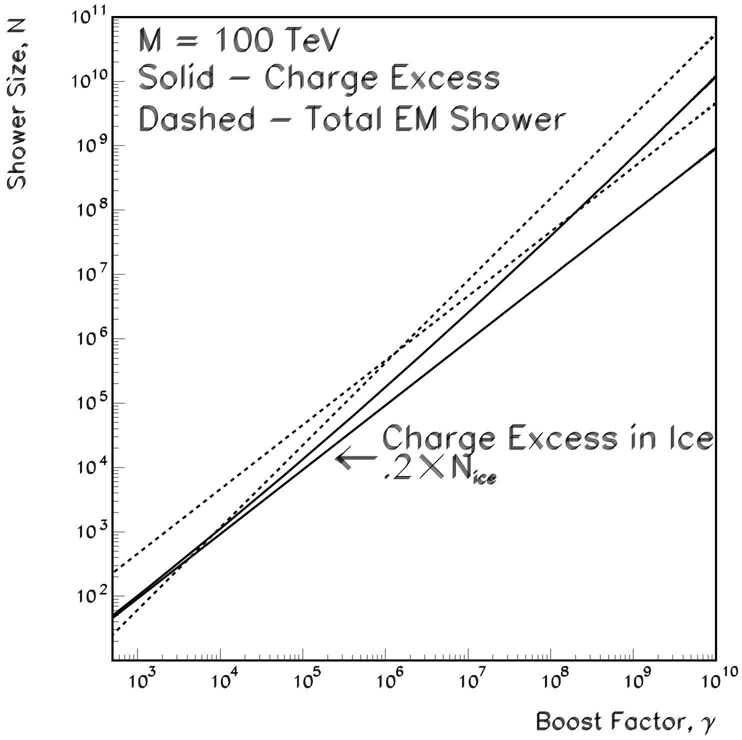

FIGURE 2. The monopole-induced quasi-steady shower size in ice for a monopole of mass 100 TeV. The shower size is the total number of electron, positrons, and photons. The dashed line $\propto \gamma$ is for pair production alone and the dashed line $\propto \gamma^{1.28}$ is for the photonuclear interaction alone. The solid lines show the electric charge excess (roughly 20% of the shower size) for pair production alone ($\propto \gamma$) and pair production plus photonuclear ($\propto \gamma^{1.28}$).

pair production and photonuclear processes separately (dashed lines) in fig. (2).

The electromagnetic shower sweeps a net charge excess from the medium into the shower of roughly 20% the shower size. For the charge excess we are again justified in using pair production alone as a lower bound and pair production plus photonuclear as an upper bound. This is reflected in fig. (2) by plotting pair production alone (the solid curve $\propto \gamma$) and by plotting pair production plus the photonuclear interaction (the solid curve $\propto \gamma^{1.28}$).

The lateral profile is approximately uniform out to a lateral cutoff given by the Molière radius

$$R_{\mathrm{M}} = 7.4\,\frac{\mathrm{g}}{\mathrm{cm}^2}\,(\frac{\xi_e}{35\mathrm{g/cm}^2})\,(\frac{100\mathrm{MeV}}{E_c}), \tag{5}$$

where ξ_e is the electron radiation length. As defined, the Molière radius is independent of the incident primary energy, being determined only by the spread of low energy particles resulting from multiple Coulomb scattering. Within a distance R_{M} of the monopole path will be $\sim 90\%$ of the shower particles [18].

Monopole Cherenkov Signatures

When a charge travels through a medium with index of refraction n, at a velocity $\beta > 1/n$, Cherenkov radiation is emitted. The total power emitted in Cherenkov radiation per unit frequency ν and per unit length l by a charge Ze is given by the Frank-Tamm formula

$$\frac{d^2W}{d\nu\, dl} = \pi\alpha Z^2\nu\left[1 - \frac{1}{\beta^2 n^2}\right]. \tag{6}$$

The maximal emission of the Cherenkov light occurs at an angle $\theta_{\max} = \arccos(1/n\beta)$ where θ is measured from the radiating particle's direction. The interaction of a magnetic charge with bulk matter requires the replacement of factors of ϵ with the Maxwell dual factors μ. But μ and ϵ are related by the index of refraction. The replacement in the electric charged–particle interaction formulae (for $Z = 1$) adequate for magnetic monopoles is $\alpha \to n^2/4\alpha$, and leads to an enhancement factor of 4700 for monopoles interacting in vacuum and 8300 for monopole interactions in water. However, in matter a relativisitic monopole is accompanied by an extensive cloud of charged particles it continually produces, so the difference in monopole electromagnetic interactions caused by the index of refraction factor is totally obscured.

The monopole-induced shower also contributes to the Cherenkov signal. In particular, the electric charge excess (of roughly 20% the shower size as shown in fig. (2)) will emit coherent Cherenkov for radio wavelengths, $\lambda >> R_{\mathrm{M}}$. For coherent radio–Cherenkov the Z^2 factor could be large, with $Z^2 \lesssim 10^{18}$, while the shower size is expected to remain roughly constant as the monopole traverses a large–scale ($\sim$ km^3) detector. Thus, a monopole signature event is clearly distinct from that of a neutrino event in the RICE array or similar large–scale detectors. The non–detection of a monopole event after one year of observation in a $\sim$ km^3 detector can, conservatively, set a flux limit of

$$F_M \ \lesssim\ 10^{-18}\ \mathrm{cm}^{-2}\ \mathrm{sec}^{-1}\ \mathrm{sr}^{-1} \tag{7}$$

which is significantly below the Parker limit.

Earth Tomography with Relativistic Monopoles

Direct knowledge about the composition and density of the Earth's interior is lacking. Analysis of the seismic data is currently the best source of information about the Earth's internal properties [19]. However, another potential probe would be the study of highly penetrating particles which could pass through the Earth's interior and interact differently depending upon the composition and density of material traversed. Thus, it may be possible to directly measure the density profile of the Earth's interior [20]. Over a range of masses, $M \sim 10^{4\pm1}$ TeV, and initial kinetic energies, monopoles can pass through the Earth's interior and emerge with relativistic velocities and, therefore, function as such probe. See [14] for more details.

BARYONIC–MONOPOLE AIR SHOWERS

The natural acceleration of monopoles to energies above the GZK cutoff at $E_{GZK} \sim 5\times10^{19}$ eV, and the allowed abundance of a monopole flux at the observed super–GZK event rate motivates us to ask whether monopoles may contribute to the super–GZK events. As a proof of principle, we have studied a simple model of a baryonic–monopole interaction in air which produces a shower similar to that arising from a hadronic primary. To mimic a hadron–initiated shower the baryonic–monopole must transfer nearly all of its energy to the shower over roughly a hadronic interaction length, $\lambda_0 \sim 80$ g cm^{-2}. The large inertia of a massive monopole makes this impossible if the cross–section is typically strong, $\sim$ 100 mb [21]. The cross–section we seek needs to be much larger.

We model our arguments on those of [11] where three $q-$monopoles are confined by Z_3 strings of color–magnetic flux to form a color–singlet baryonic–monopole. We further assume that 1) the cross–section for the interaction of the baryonic–monopole with a target nucleus is geometric; in its unstretched state (before hitting the atmosphere) the monopole's cross–section is roughly hadronic, $\sigma_0 \sim \Lambda^{-2}$ (where $\Lambda \equiv \Lambda_{QCD}$); 2) each interaction between the baryonic–monopole and an air nucleus transfers an $O(1)$ fraction of the exchanged energy into stretching the chromomagnetic strings; 3) the chromomagnetic strings can only be broken with the formation of a monopole–antimonopole pair, a process which is highly suppressed and therefore ignored; other possible relaxation processes of the stretched string are assumed to be negligible; 4) the energy transfer per interaction is soft, $\Delta E/E \equiv \eta \sim \Lambda/M$.

The color–magnetic strings have a string tension $\mu \simeq \Lambda^2$. Therefore, when $O(1)$ of the energy transfer $(\gamma\Lambda)$ stretches the color–magnetic strings (assumption 2), the length $l \sim \Lambda^{-1}$ increases by $\delta l = dE/\mu$, so that the fractional increase in length is $\delta l/l = \gamma$. Consequently, the geometrical cross–section grows $\propto \gamma\Lambda^{-2}$ after each interaction. The energy loss for baryonic-monopoles can then be approximated as

$$\frac{dE}{dx}(x) \;\simeq\; -\frac{\gamma\,\Lambda}{\lambda(x)} \;\simeq\; -\gamma\,\Lambda\, n_N\, \sigma(x), \tag{8}$$

where the strong cross–section $\sigma(x)$ is explicitly a function of column depth x and n_N is the number density of target nucleons. From assumption (4) we infer that the total number of monopole-nucleus interactions required to transfer most of the incoming kinetic energy is roughly η^{-1}. From the above discussion, the geometrical cross–section after n interactions is

$$\sigma_n \sim \frac{1+\sum_{i=1}^{n}\gamma_i}{\Lambda^2} = \frac{1+n\gamma}{\Lambda^2}\,, \tag{9}$$

where we have approximated $\gamma_n \sim (1-\eta)^n\,\gamma \sim \gamma$. The mean-free-path $\lambda \equiv 1/\sigma n_N$ after the n-th interaction is therefore

$$\lambda_n \sim \frac{\Lambda^2}{n_N \gamma n}, \qquad n \geq 1\,, \tag{10}$$

and the total distance traveled between the first interaction and the $(\eta^{-1})^{\rm th}$ interaction is

$$\Delta X \sim \sum_{n=1}^{\eta^{-1}} \lambda_n \;\sim\; \frac{\Lambda^2}{n_N\,\gamma}\ln\left(\frac{M}{\Lambda}\right) \;<<\lambda_0 \tag{11}$$

for $\eta^{-1} \gg 1$. Thus the stretchable chromomagnetic strings of the baryonic–monopole provide an example of a very massive monopole which nevertheless transfers O(1) of its kinetic energy to an air shower over a very short distance. In conclusion, the baryonic–monopole's air–shower signature roughly mimics that of a hadronic primary.

ACKNOWLEDGMENTS.

This work was supported in part by the U.S. Department of Energy grants no. DE-FG05-86ER40272 (SDW), DE-FG05-85ER40226 (TWK & TJW), and the Vanderbilt University Research Council.

REFERENCES

1. E. N. Parker, Astrophys. J. **160**, 383 (1970).
2. N.A. Porter, Nuovo Cim. **16**, 958 (1960); E. Goto, Prog. Theo. Phys. **30**, 700 (1963).
3. T.W. Kephart and T.J. Weiler, Astropart. Phys. **4** 271 (1996); Nucl. Phys. (Proc. Suppl.) **51B**, 218 (1996).
4. T. W. Kibble, Phys. Rept. **67**, 183 (1980), and references therein.
5. S. F. King and Q. Shafi, Phys. Lett. **B422**, 135 (1998)[hep-ph/9711288].
6. D.K. Hong, J. Kim, J.E. Kim, and K.S. Soh, Phys. Rev. **D27**, 1651 (1983).
7. N. G. Deshpande, B. Dutta and E. Keith, Nucl. Phys. Proc. Suppl. **52A**, 172 (1997)[hep-ph/9607307]; Phys. Lett. **B388**, 605 (1996)[hep-ph/9605386]; Phys. Lett. **B384**, 116 (1996)[hep-ph/9604236].
8. P. H. Frampton and B. Lee, Phys. Rev. Lett. **64**, 619 (1990); P. H. Frampton and T. W. Kephart, Phys. Rev. **D42**, 3892 (1990).
9. C.L. Gardner and J.A. Harvey, Phys. Rev. Lett. **52,** 879 (1984).
10. T. Vachaspati, Phys. Rev. Lett. **76**, 188 (1996)[hep-ph/9509271]; H. Liu and T. Vachaspati, Phys. Rev. **D56**, 1300 (1997)[hep-th/9604138].
11. A. S. Goldhaber, Phys. Rept. **315**, 83 (1999)[hep-th/9905208].
12. For a review see P. P. Kronberg, Rept. Prog. Phys. **57**, 325 (1994).
13. D. Ryu, H. Kang, and P.L. Biermann, Astron. & Astrophys. **335**, 19 (1998)[astro-ph/9803275].
14. S. D. Wick, T.W. Kephart, T.J. Weiler, and P.L. Biermann, submitted to Astropart. Phys. [astro-ph/0001233].
15. G. Giacomelli, in: *Theory and Detection of Magnetic Monopoles in Gauge Theories,* ed. N. Craigie p.407 (Singapore: World Scientific Publishing Co., 1986).
16. S. P. Ahlen, Rev. Mod. Phys. **52,** 121 (1980).
17. S. Iyer Dutta, M. H. Reno, I. Sarcevic, and D. Seckel, [hep-ph/0012350].
18. Particle Data Group, Phys. Rev. D **50**, 1173 (1994). Prentice-Hall, 1952). 485 (1940).
19. T. Lay and T. C. Wallace, *Modern Global Seismology* (New York: Academic Press, 1995); Properties of the Solid Earth, in Rev.Geophys. **33,** (1995).
20. This idea has been exploited in neutrino physics as neutrinos are sufficiently weakly interacting to pass through the earth largely unimpeded for neutrino energies $\lesssim 10^{15}$ eV.
21. R.N. Mohapatra and S. Nussinov,Phys. Rev. **D57**, 1940 (1998); in I.F.M. Albuquerque, G. Farrar, and E.W. Kolb, Phys. Rev. **D59**, 015021 (1999) it is noted that a baryon mass above 10 GeV produces a noticeably different shower profile, and a baryon mass above 50 GeV is so different as to be ruled out.